Forest Ecology and Management 593 (2025) 122918

Contents lists available at ScienceDirect

Forest Ecology and Management

journal homepage: www.elsevier.com/locate/foreco

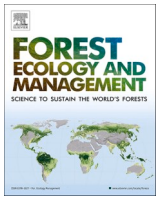

# Promoting effect of tree mixture on litter quality and microbial diversity governs microbial necromass accrual in previously degraded soils

Cui Deng [a], Maokui Lyu [a,b,*], Jordi Sardans [c,d], Josep Peñuelas [c,d], Yuming Lu [a], Yongmeng Jiang [a], Yusheng Yang [a,b], Jinsheng Xie [a,b,*]

[a] Key Laboratory for Humid Subtropical Eco-geographical Processes of the Ministry of Education, Fujian Normal University, Fuzhou 350117, China
[b] Sanming Forest Ecosystem National Observation and Research Station, Fujian Normal University, Sanming 365002, China
[c] CSIC, Global Ecology Unit CREAF-CSIC-UAB, Cerdanyola del Vallès, Catalonia 08913, Spain
[d] CREAF, Cerdanyola del Vallès, Catalonia 08913, Spain

ARTICLE INFO

*Keywords:*
Tree species mixture
Microbial necromass carbon
Degraded ecosystems
Microbial diversity and functioning
Litter quality

ABSTRACT

Introducing broadleaf tree species into pine forests has been widely adopted as a strategy to mitigate forest degradation and enhance soil carbon sequestration. However, the microbial-mediated mechanisms underlying the effects of mixed coniferous-broadleaf forests on soil carbon sequestration in degraded forest ecosystems remain inadequately elucidated. This study investigated two previously degraded sites in southern China, presenting vegetation cover since 1981 and 2000, respectively. Within these sites, single Pine (*Pinus massoniana*) plantations and mixed plantations of pine and broadleaf species (Pine+*Schima superba*) were established as part of restoration efforts. Amino sugars were quantified as biomarkers of topsoil (0–10 cm) microbial necromass, and microbial community diversity and structure were assessed via high-throughput sequencing techniques (16S rRNA and ITS sequencing) and phospholipid fatty acids analysis. Our results showed that tree mixture increased soil microbial necromass, with the fungal necromass increasing more rapidly than bacterial necromass, suggesting that fungal necromass rapidly responds to tree species mixture effects, but bacterial necromass drives the sustained accumulation of microbial necromass C in the later restoration stages. Furthermore, mixed plantation soils yield higher bacterial α-diversity (Chao1), and ectomycorrhizal fungi abundance, all of which positively influence microbial necromass accumulation. Structural equation modelling results showed that tree mixture strengthens the integrated effects of litter quality and soil nitrogen status on microbial community composition (16S rRNA and ITS sequencing) and functions (FUNGuild) and thus enhancing microbial necromass. Importantly, this ecological restoration effect shifted microbial necromass regulation from dual independent pathways (physicochemical vs. microbial factors) to an integrated soil-microbial feedback loop, with mixed pine-broadleaf plantations enhancing the interaction between soil nutrient availability and microbial functional diversity to promote microbially-derived carbon accrual in soils. These findings demonstrate that introducing tree species with high-quality litter constitutes an effective vegetation restoration strategy, simultaneously accelerating soil organic matter sequestration in degraded pine forest ecosystems.

## 1. Introduction

Land degradation has become a critical global issue, affecting approximately 30 % of terrestrial ecosystems, with particularly severe impacts in tropical and subtropical biomes (Lal et al., 2015; Coban et al., 2022). This crisis undermines soil health, reduces ecosystem services, and hinders soil organic matter (SOM) accumulation, thereby compromising climate change mitigation efforts (Chazdon, 2008; Xie et al., 2013; Lal et al., 2015). Restoring degraded lands through biomass enhancement and SOM recovery is increasingly recognized as a cost-effective strategy for ecosystem recovery (Bukoski et al., 2022; Lal et al., 2015). Notably, degraded soils exhibit greater carbon (C) sequestration potential than non-degraded soils, offering unique ecological opportunities (Xie et al., 2013; Lal et al., 2015; Lyu et al., 2019). However, large-scale monoculture plantations (e.g., single-species pine stands) have proven efficient in promoting SOM

* Corresponding authors at: Key Laboratory for Humid Subtropical Eco-geographical Processes of the Ministry of Education, Fujian Normal University, Fuzhou 350117, China.
*E-mail addresses:* 228lmk@163.com (M. Lyu), jshxie@163.com (J. Xie).

https://doi.org/10.1016/j.foreco.2025.122918
Received 26 March 2025; Received in revised form 14 May 2025; Accepted 10 June 2025
Available online 17 June 2025

accumulation remains problematic (Berthrong et al., 2009; Bukoski et al., 2022; Huang et al., 2018). Thus, developing effective strategies to accelerate SOM restoration in degraded ecosystems remains a pressing challenge.

Emerging evidence demonstrates that mixed plantations enhance plant productivity and SOM accumulation through diversified litter inputs, yet the mechanistic pathways underlying these synergistic effects remain debated (Chen et al., 2020; Hua et al., 2022; Feng et al., 2022). Contemporary research implicates microbially-derived C as the predominant SOM constituent (>50 %), with litter quality (C:nitrogen and lignin:nitrogen ratios) mediating microbial necromass formation via nutrient-mediated shifts in microbial community structure and C use efficiency (Liang et al., 2019; Wang et al., 2021; Li et al., 2024). Compared to monoculture systems, tree species mixing elevates litter heterogeneity, improves soil nutrient availability, and boosts microbial biomass — factors hypothesized to accelerate microbial turnover and subsequent synthesis of persistent SOM through complementarity effects (Lange et al., 2015; Huang et al., 2018; Prommer et al., 2020). Nevertheless, the specific interspecific interactions governing these soil-microbial feedbacks in degraded ecosystems remain unclear.

The formation of microbially-derived SOM fundamentally depends on microbial processing of heterogeneous litter substrates, as posited by the resource heterogeneity hypothesis (Gessner et al., 2010). While abiotic factors contribute to initial SOM stabilization, microbial decomposition efficiency determines ultimate C sequestration potential — particularly through functional diversity-mediated nutrient liberation from complex organic compounds (Shao et al., 2021; Coban et al., 2022). Field observations reveal that mixed pine-broadleaf systems exhibit superior litter quality and microbial diversity compared to monocultures, suggesting vegetation restoration strategies can engineer microbial communities to optimize SOM formation (Lyu et al., 2019; Lu et al., 2023; Allsup et al., 2023). Though operational mechanisms require systematic verification, this conceptual framework positions microbial community dynamics as the critical nexus between plant diversity and SOM accrual in degraded lands.

Southern China's subtropical ecosystems represent the nation's second-largest degraded area, surpassed only by the Loess Plateau, with historical deforestation of evergreen broadleaf forests triggering chronic nutrient depletion and shallow soil organic C (SOC) stocks (Xie et al., 2013; Bai et al., 2020). Government-led afforestation initiatives since the 1980s established extensive *Pinus massoniana* monocultures, achieving modest yet ecologically insufficient SOC accumulation over three decades (Lyu et al., 2019; Deng et al., 2023). This persistent limitation stems from the interplay of climatic stressors (high precipitation/temperature regimes) and edaphic constraints in hilly terrain, compounded by monospecific plantation management (Cao et al., 2009; Zhao et al., 2013).

To address this ecological impasse, we established a chronosequence experiment comparing single-pine stands with mixed Pine-*Schima superba* plantations across restoration stages. We hypothesised that: (H1) broadleaf admixture enhances total SOC through rapid bacterial-derived C accrual, leveraging bacterial communities' heightened sensitivity to nitrogen-rich litter inputs relative to fungal counterparts (Wang et al., 2021; Hu et al., 2023); and (H2) tree species mixing amplifies microbial diversity-microbial necromass feedbacks, creating self-reinforcing SOC sequestration mechanisms. By quantifying microbial necromass dynamics throughout forest developmental stages, we elucidate the optimal timing for C capture and identify key drivers (litter quality, nutrient stoichiometry, microbial functional traits) governing microbially-mediated SOC accumulation. These insights advance ecological restoration paradigms by bridging vegetation composition with belowground C stabilization processes in degraded subtropical landscapes.

## 2. Materials and methods

### 2.1. Experimental design

This study was conducted at the Hetian Erosion Research Station (25°33'N, 116°18'E) in Changting County, Fujian Province, China (Fig. S1). Situated in a subtropical monsoon climate zone, the station receives an average annual precipitation of 1696 mm with a mean air temperature of 18.3°C based on meteorological records spanning 1956–2015. The experimental site occupies undulating terrain at elevations ranging from 300 to 400 m above sea level. The dominant soil type is classified as humic planosols (Soil Survey Staff, 2014), derived from medium- to coarse-grained granite parent material (Lyu et al., 2019). Historically, this area supported subtropical evergreen broadleaf forests that experienced severe degradation due to prolonged anthropogenic disturbances. Since the 1980s, systematic vegetation cover (VC) initiatives led by government programs have been implemented, including revegetation of barren slopes and strict regulation of human activities. These conservation measures have proven effective in controlling soil erosion rates, as documented by longitudinal monitoring studies (Xie et al., 2013; Lyu et al., 2019).

The study employed a stratified randomized complete block design to investigate vegetation restoration trajectories in chronosequential ecosystems. Within the government-initiated restoration corridor (established 1980-present), we selected two distinct restoration blocks differentiated by initiation year (VC-1981 vs. VC-2000) as temporal strata, each representing homogeneous edaphic conditions (Typic Dystrudepts, USDA Soil Taxonomy) with $< 5$ % slope variation. Each 50-ha block contained eight 400 $m^2$ experimental units systematically distributed across four topographic positions (upper, middle, lower slope, riparian) to control microhabitat variability. Through restricted randomization within blocks, we assigned four replicates per treatment (single pine vs. pine+*Schima superba*) to independent 20 × 20 m plots, ensuring $\geq$ 200 m buffer zones between experimental units to eliminate edge effects. This design yielded 16 spatially explicit treatment plots (2 restoration stages × 2 vegetation types × 4 replicates) with rigorous counterbalancing of aspect and solar exposure covariates (Fig. S1). Geostatistical analysis confirmed no significant pre-treatment differences in baseline SOC stocks (Lyu et al., 2019). In the two forest stands with different restoration ages (VC-1981 and VC-2000), *Pinus massoniana* exhibited distinct planting densities across stand types. The monoculture stands contained 3475 stems $ha^{-1}$ in VC-2000 and 1400 stems $ha^{-1}$ in VC-1981 for single pine plantations. In mixed plantations combining *P. massoniana* with *Schima superba*, pine densities were recorded at 3200 stems $ha^{-1}$ (VC-2000) and 1625 stems $ha^{-1}$ (VC-1981), while the companion species *S. superba* showed corresponding densities of 1275 stems $ha^{-1}$ and 700 stems $ha^{-1}$ for the respective restoration years. Tree height and diameter at breast height (DBH) metrics are presented in Table 1.

The study site was intentionally selected in a historically homogenous degraded ecosystem. Before afforestation (1981), the entire watershed had experienced severe soil erosion with completely denuded vegetation (Fig. S2). Post-1981 plantations were established through standardized statewide erosion control protocols, ensuring uniform soil conditions (Xie et al., 2013; Lyu et al., 2019; Deng et al., 2023).

### 2.2. Sampling and laboratory analysis

Four randomly placed traps (0.16 $m^{-2}$ each) were used to collect forest floor litter in each plot. The litter samples were transported to the laboratory, oven-dried at 65°C for 72 h, and weighed. Litter C and nitrogen (N) concentrations were determined using an elemental analyzer (Elemental Vario EL III, Germany).

In August 2020, soil samples (0–10 cm depth) were randomly collected from both the single pine and pine+*S. superba* plots. Soil samples were stored on ice and transported to the laboratory for

**Table 1**
Stand characteristics and soil properties (0–10 cm). results are mean ± standard deviation ($n = 4$). the $p$ value with a test of significance of the generalized linear model (GLM) indicates the effects of stand age, species mixture, and their interaction on plant and soil properties. Vc-1981 and VC-2000 represent vegetation cover established in 1981 and 2000, respectively.

| | | VC-2000 | | VC-1981 | | Effect (*P*-value) | | |
|---|---|---|---|---|---|---|---|---|
| | Tree species | Single-Pine | Pine+*S. superba* | Single-Pine | Pine+*S. superba* | Age | Mixture | Age×Mixture |
| Height (m) | *Pinus massoniana* | 9.4 (0.3) | 9.8 (0.9) | 6.7(0.5) | 10.9(0.2) | **0.011** | **< 0.001** | **< 0.001** |
| | *Schima superba* | | 6.2 (1.0) | | 8.9(0.8) | | | |
| DBH (cm) | *Pinus massoniana* | 9.6 (1.0) | 10.9 (0.9) | 11.0(1.3) | 14.3(1.4) | **0.001** | **0.002** | 0.112 |
| | *Schima superba* | | 6.7 (1.3) | | 14.1(2.4) | | | |
| Litter C stock (Mg ha$^{-1}$) | | 32.8(7.06) | 44.44(4.26) | 43.81(1.51) | 33.25(6.40) | 0.974 | 0.840 | **0.001** |
| Litter N stock (Mg ha$^{-1}$) | | 0.3(0.07) | 0.63(0.06) | 0.39(0.08) | 0.65(0.07) | 0.140 | **<0.001** | 0.328 |
| Soil bulk density (g cm$^{-3}$) | | 1.26 (0.11) | 1.00 (0.31) | 1.17(0.14) | 1.19(0.08) | 0.589 | 0.217 | 0.147 |
| Soil pH | | 4.38 (0.27) | 4.00 (0.10) | 4.24(0.13) | 4.20(0.04) | 0.745 | **0.019** | **0.048** |
| Total N (g kg$^{-1}$) | | 0.91 (0.24) | 0.94 (0.23) | 0.67(0.14) | 1.34(0.13) | 0.399 | **0.004** | **0.006** |
| Soil C:N | | 14.60 (2.73) | 18.69 (0.63) | 17.54(1.23) | 17.08(0.70) | 0.416 | **0.040** | **0.014** |
| Total Phosphorus (g kg$^{-1}$) | | 0.13 (0.03) | 0.11 (0.02) | 0.12(0.03) | 0.21(0.03) | **0.014** | **0.025** | **0.003** |
| Dissolved organic C (mg kg$^{-1}$) | | 59.51 (7.12) | 70.96 (16.09) | 70.78(16.86) | 74.05(14.01) | 0.327 | 0.316 | 0.571 |
| Dissolved organic N (mg kg$^{-1}$) | | 0.97 (0.51) | 3.65 (1.17) | 2.38(0.30) | 8.85(2.24) | **<0.001** | **<0.001** | **0.013** |
| Microbial biomass C (mg kg$^{-1}$) | | 140.01(23.64) | 177.46(9.57) | 151.06(35.93) | 221.28(29.94) | 0.062 | **0.002** | 0.242 |
| Microbial biomass N (mg kg$^{-1}$) | | 21.09(1.20) | 18.82(8.37) | 19.36(5.82) | 35.80(7.02) | **0.030** | **0.042** | **0.011** |

DBH: diameter at breast height, C:N: carbon to nitrogen ratio.

analysis. After removing gravel, roots, and debris (> 2 mm) by sieving, the soil was processed as follows: Microbial community composition was assessed via phospholipid fatty acids (PLFAs) analysis. Subsamples were stored at −80°C for future DNA extraction. The remaining soil was air-dried and sieved (0.149 mm mesh) for determination of total soil C, total N (TN), and total phosphorus (TP) concentrations, as well as the concentration of amino sugars. Soil pH was measured in a soil-deionized water mixture (the soil: water ratio was 1:2.5 w/v). Soil C and N concentrations were analyzed using the elemental analyzer (Elemental Vario EL III, Germany). SOC stock (SOCS, Mg ha$^{-1}$) was calculated as:

$$SOCS = SOC \times BD \times PSS \times SD/10 \quad (1)$$

Where SOC is the content of SOC (g kg$^{-1}$), BD is the bulk density (g cm$^{-3}$), PSS is the proportion of sieved soil (%), and SD is the soil depth (cm).

Soil TP was s determined via colorimetric method using an alkaline oxidation digestion procedure (Dick and Tabatabai, 1977). Dissolved organic C (DOC) and dissolved organic N (DON) were extracted with deionized water (Jones and Willett, 2006). The supernatant was analyzed for TP and DON using a continuous flow analyzer (Skalar San$^{++}$, The Netherlands), and DOC was measured with a Total Organic Carbon Analyzer (Shimadzu, Japan).

### 2.3. Soil microbial parameters

Microbial DNA was extracted from (> 1 g) fresh soil using the OMEGA E.Z.N.A.® Soil DNA Kit (Omega Bio-Tek, Inc., Norcross, GA, USA) following the manufacturer's protocol. DNA concentration was determined using a NanoDrop 2000 UV/Vis spectrophotometer (Thermo Fisher, USA). Bacterial 16S rRNA (V3-V4 region) was amplified using the primers 338 F/806 R (Xu et al., 2016) under the following PCR conditions: Denaturation at 94°C for 3 min; then 30 cycles of denaturation at 94°C for 10 s, annealing at 55°C for 15 s, and elongation at 72°C for 30 s; and finally, a hold at 72°C for 7 min. The fungal ITS1 region was amplified with primers: ITS1F/ITS2R (Adams et al., 2013). The PCR reaction included: Denaturation at 95°C for 5 min; followed by 35 cycles at 95°C for 1 min, annealing at 53°C for 45 s, and elongation at 72°C for 1 min; and finally, extension at 72°C for 7 min. Sequencing was performed on an Illumina MiSeq platform by Beijing Auwigene Tech, China. Raw reads were quality-filtered using QIIME (Caporaso et al., 2010), discarding sequences with length < 100 bp or quality score < 25. Paired-end reads were assembled: 16S rRNA reads were joined using FLASH, while ITS reads were joined using Fastq Join (Magoč and Salzberg, 2011). The remaining high-quality sequences were clustered into OTUs at 97 % similarity using UPARSE (Edgar, 2013). Ectomycorrhizal (EcM) fungi OTUs were predicted via FUNGuild (ITS data).

Microbial biomass C (MBC) and N (MBN) were measured by chloroform fumigation (Vance et al., 1987). Phospholipid fatty acids (PLFAs) analysis quantified key microbial groups (White et al., 1979). Indicator groups included: fungi (18:2ω6) (Frostegård et al., 2011; Lyu et al., 2019), bacteria (14:0iso, 15:0anteiso, 15:0iso, 16:0iso, 17:0anteiso, 17:0iso, 16:1ω5, 16:1ω9c, 16:1ω7c, 18:1ω7c, 18:1ω5c, 19:0 cycloω7c, 17:0 cycloω7c) (Frostegård et al., 2011; Lü et al., 2015). and actinomycete (16:0 10 methyl, 17:0 10 methyl, 18:0 10 methyl) (Frostegård et al., 2011; Lü et al., 2015). The ratio of fungal to bacterial biomass (F:B ratio) was calculated from the ratio of fungal to bacterial PLFAs. For further details, please see Lü et al. (2015). We studied the enzymes involved in the degradation of C and N in soil, including β-1,4-glucosidase (βG, EC3.2.1.21), cellobiohydrolase (CBH, EC3.2.1.91) and β- 1, 4-N-acetylglucosaminidase (NAG, EC 3.1.6.1) (Saiya-Cork et al., 2002). The enzyme data were then used to calculate microbial C use efficiency. Although soil enzyme assays have been widely debated (Margenot and Wade, 2023), they are still widely used and offer valuable insights.

Microbial C use efficiency (CUE) was measured and calculated according to the method of Sinsabaugh et al. (2016).

$$CUE_{C:N} = CUE_{\max}[S_{C:N}/(S_{C:N} + K_N)] \quad (2)$$

$$S_{C:N} = (1/EEA_{C:N})(B_{C:N}/L_{C:N}) \quad (3)$$

$S_{C:N}$ indicates the extent to which enzyme activity offsets the disparity between the stoichiometry of available microbial resources (DOC:DON ratio) and microbial biomass (Sinsabaugh et al., 2016; Chen et al., 2018). $CUE_{max}$ is the upper limit of microbial growth efficiency based on thermodynamic constraints (0.6). The value of $K_N$ is set to 0.5 (Sinsabaugh et al., 2016). $B_{C:N}$ is the C:N ratio of microbial biomass, $EEA_{C:N}$ is the ratio of enzyme activity (βG+CBH):NAG. $L_{C:N}$ is the C:N ratio of DOC:DON (Sinsabaugh et al., 2016; Chen et al., 2018).

Amino sugars were extracted to quantify soil microbial necromass C (Zhang and Amelung, 1996). Briefly, hydrolysis: freeze-dried, sieved soil was hydrolyzed with 6 M HCl at 105°C for 8 h. Internal standard: 0.1 mL inositol was added. The solution was filtered through a 0.45-diameter glass fiber membrane, dried using a rotary evaporator (45℃), and re-dissolved in deionized water. The pH was adjusted to 6.6–6.8 (1 M KOH/0.01 M HCl). Finally, derivatization: converted to a malononitrile derivative, extracted with dichloromethane. The amino sugar derivatives were separated on an Agilent 6890 A gas chromatograph (GC, Agilent Technologies, USA) equipped with a flame ionization detector

(FID) and a DB-1 capillary column (30 m × 0.32 mm × 0.25 μm). The total amino sugar content represents the sum of the four amino sugars: galactosamine (GalN), glucosamine (GluN), mannosamine (ManN), and muramic acid (MurA) (Joergensen, 2018).

Soil microbial necromass C was calculated using the following equation:

$$Bacterial\ residual\ C\ (mgkg^{-1}) = MurN \times 45 \quad (4)$$

$$Fungal\ residual\ C\ (mgkg^{-1}) = (nmol\ CluN - 2 \times nmol\ MurN) \times 179.2 \times 9 \quad (5)$$

The following conversion values were used: 45 to convert bacterial MurA to bacterial necromass C, and nine to convert fungal GluN to fungal necromass C (Appuhn and Joergensen, 2006). A 1:2 ratio of MurA to GluN was assumed for bacterial cells, where 179.2 is the molecular weight of GluN. The total microbial necromass C was calculated as the sum of bacterial necromass C and fungal residual necromass C.

### 2.4. Statistical analysis

The Chao1 estimator was used to assess $\alpha$-diversity (richness). A generalized linear model (GLM) was evaluated the effects of stand age, species mixture, and their interaction on stand characteristics (tree height, DBH), soil physicochemical properties (bulk density, pH, C:N ratio, DOC, DON, SOC, TN, TP), litter attributes (forest floor litter mass, litter C stock, litter C:N stock, litter C:N), soil C stocks, microbial necromass C (total, fungal, bacterial), microbial properties (abundance of bacteria, fungi, EcM fungi, and bacterial and fungal $\alpha$-diversity). Effects were considered significant at $P < 0.05$

Linear regression assessed the relationship between microbial necromass (total, fungal, bacterial) and SOC stock. Before analysis, SOC stock, total microbial necromass, fungal necromass, and bacterial necromass were normalized. A slope closer to 1 indicates that the independent variables (total, fungal, and bacterial necromass) can better explain SOC stock variability.

A linear mixed-effects model identified the most significant predictors. To assess the impacts of microbial traits on microbial necromass, a hierarchical partitioning model based on the R package 'glmm.hp' (Lai et al., 2022) quantified the contributions of bacterial and fungal α-diversity, fungal and bacterial PLFAs, EcM fungi, and C-degrading enzymes. After model optimization, four key variables were retained: bacterial α-diversity, EcM fungi, C-degrading enzyme, and CUE. Partial correlation analysis (controlling for litter and soil properties) further examined microbial diversity, abundance, and metabolic characteristics on microbial necromass (Doetterl et al., 2015). During the analysis, we mainly used the R package Hmisc to calculate the regular Spearman correlation coefficients, the ppcor package (pcor.test function) to calculate Spearman's partial correlation coefficients, and the ggplot2 package for visualization. Pearson coefficients and Mantel tests were used to evaluate relationships between microbial necromass C and microbial community structure, litter, and soil physicochemical properties. Partial mantel tests used the "mantel.partial" function (999 permutations) in the "vegan" R package (Wu et al., 2021). Random forest (RF, "randomForest" package) model was separately analyzed for single pine and pine+*S. superba* treatments (Breiman, 2001). In the RF models, litter, microbial, and soil physicochemical properties served as predictors of microbial necromass C to estimate microbial contributions to SOC formation. Variance partitioning analysis quantified the relative importance of predictors.

Structural equation modeling (SEM, AMOS 21.0) explored environmental drivers of microbial necromass C accumulation. Model fit was assessed using $\chi^2$ ($0 \leq \chi^2 \leq 2$), *P*-value ($0.05 \leq P \leq 1.00$), RMSEA ($0 \leq$ RMSEA $\leq 0.05$), goodness-of-fit index (GFI $> 0.90$), and Akaike information criterion (AIC) value. The litter, microbial, and soil physicochemical properties were represented by their PC1 scores.

## 3. Results

### 3.1. Soil carbon stocks and microbial necromass carbon

Mixed plantations of pine + *S. superba* yeild significantly higher SOC stock ($F$=5.79, $P = 0.033$), fungal necromass C ($F$=26.58, $P < 0.001$), bacterial necromass C ($F$=5.98, $P = 0.031$), and total microbial necromass C ($F$=22.27, $P < 0.001$) compared to single pine plantations, with increases of 40.0 %, 57.8 %, 30.2 %, and 52.4 %, respectively (Fig. 1). Stand age had significant effects on SOC stocks ($F$=11.87, $P = 0.005$) and bacterial necromass C ($F$=6.32, $P = 0.027$), but no stand-age effects on fungal and total microbial necromass C (Fig. 1).

Regardless of treatment, there are significant relationships between microbial necromass and SOC, with the strongest relationships between bacterial necromass and SOC (Fig. 2c). However, analyzing the treatments separately revealed the relationship between bacterial necromass C and SOC was not significant in single pine plots whereas we observed a significant relationship between bacterial necromass and SOC in pine+*S. superba* plots (Fig. 2a, b).

### 3.2. Litter and soil physicochemical properties

Tree species mixing increased forest floor litter mass in VC-2000 stands but decreased it in VC-1981 stands (Fig. 3). Litter N stock was significantly higher in mixed plantations than in single pine plantations, leading to a lower litter C:N ratio in mixed plantations (Table 1, Fig. 3). Compared to single pine plantations, mixed plantations significantly decreased soil pH, and increased total soil P, soil C:N ratio, total N, and DON (Table 1). Overall, the quality of litter input to soil has been improved by pine mixed with *S. superba*, thereby enhancing soil nutrient status.

### 3.3. Tree species mixture effects on soil microbial properties

For microbial biomass, tree species mixture significantly increased MBC, MBN, and actinomycete, but significantly reduced the F:B ratio (Table 1 and Fig. S2). Furthermore, stand age and tree species mixture significantly interact to affect soil MBN, actinomycete, and F:B (Fig. S2). Although fungal and bacterial phospholipid fatty acid (PLFA) profiles remained statistically unaltered by mixing alone (Fig. 4ab), bacterial PLFA exhibited significant age × treatment interactions (Fig. 4b; $F = 9.05$, $P = 0.011$). For microbial diversity, tree species mixture significantly increased bacterial $\alpha$-diversity (Chao 1) but did not affect fungal $\alpha$-diversity (Fig. 4c, d). For microbial metabolism, tree species mixture significantly decreased C-degrading enzyme activity (Fig. 4e; $F$=7.10, $P = 0.021$) but increased microbial CUE (Fig. 4f; $F$=9.60, $P = 0.009$).

Tree species mixture did not affect bacterial biomass but significantly increased its diversity (Fig. 4). Although tree species mixture did not affect fungal biomass and diversity, significant shifts occurred in the key fungal taxon. For example, according to the ITS gene analysis in FUNGuild, symbiotrophs, such as EcM fungi, were more common in the mixed plantations. Overall, tree species mixture significantly increased the abundance of EcM fungi by 100.03 % on average compared with single pine plots (Fig. S3; $F$=6.43, $P = 0.026$).

### 3.4. Drivers of soil microbial necromass carbon and community composition

We observed significant negative correlations between litter C:N ratio and microbial necromass (including both fungal and bacterial necromass), while bacterial α-diversity showed significant positive correlations with microbial necromass accumulation, particularly with bacterial-derived necromass (Fig. 5). Multivariate analyses revealed distinct drivers of microbial necromass between monoculture and mixed plantations. In single pine stands, EcM fungi dominated necromass accumulation (86 % variance explained), while bacterial α-diversity

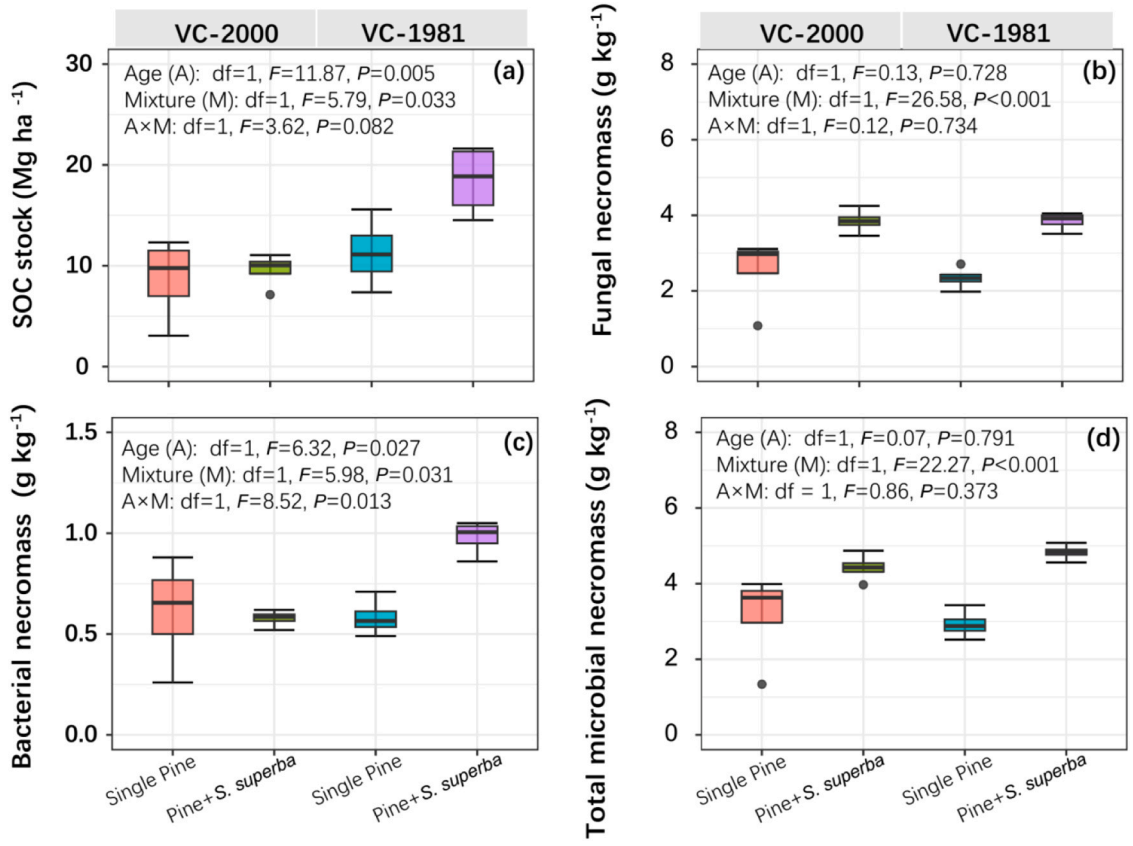


**Fig. 1.** Soil carbon stock (a), fungal necromass carbon (b), bacterial necromass carbon (c) and total microbial necromass carbon (d) at the top of 0–10 cm soils. The effects of stand age (A), species mixture (M), and their interaction (A × M) on soil carbon stock, fungal necromass carbon, bacterial necromass carbon and total microbial necromass carbon are presented as the *p* value with a test of significance of generalized linear model (GLM). VC-1981 and VC-2000 represent vegetation cover (VC) established in 1981 and 2000, respectively.

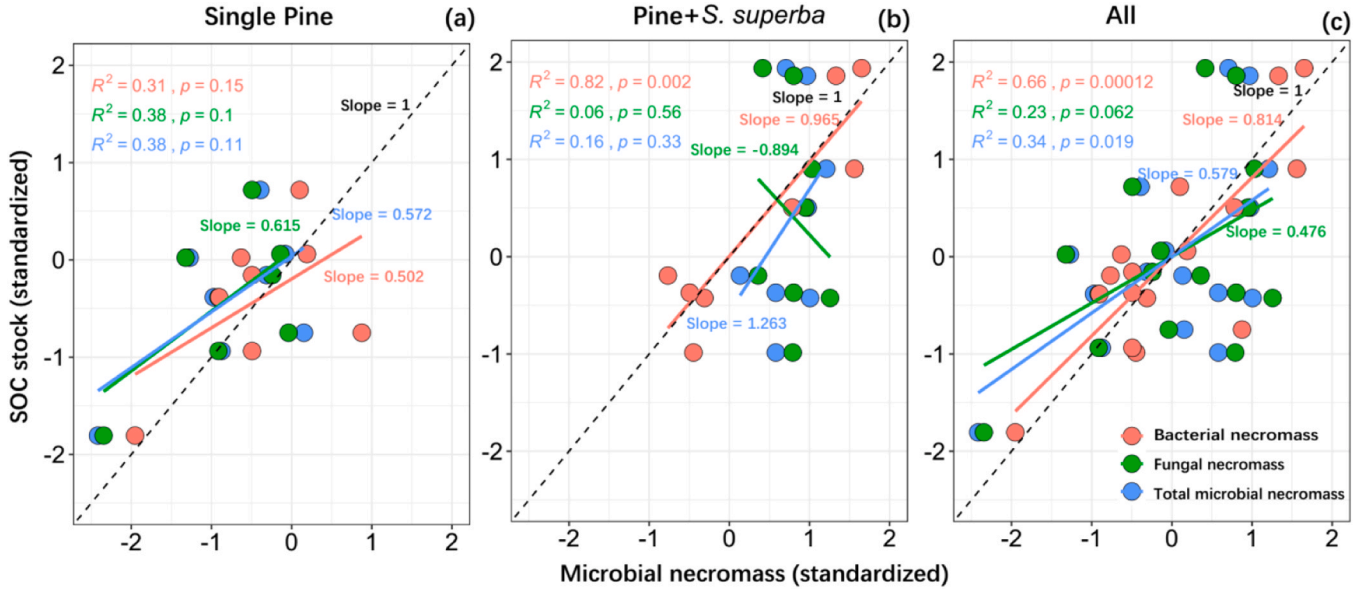


**Fig. 2.** The regression analysis between soil organic carbon (SOC) stock and total microbial necromass (blue), fungal necromass (green), and bacterial necromass (red) in single pine (a), pine+*S. superba* (b), and all stands (c). a slope closer to 1 indicates the highest predictor for changes in SOC stock.

emerged as the primary driver in mixed plantations (55 % variance explained), with microbial traits explaining 42 % and 78 % of total variance respectively (Fig. 6). Structural equation modeling demonstrated mixed plantations enhanced integrated soil-microbial-litter interactions, increasing necromass C explanatory power to 75 % versus monocultures 61 % (Fig. 7cd). Partial Mantel tests identified stronger litter-microbe linkages in mixed stands, particularly bacterial necromass associations with community composition, absent in monocultures

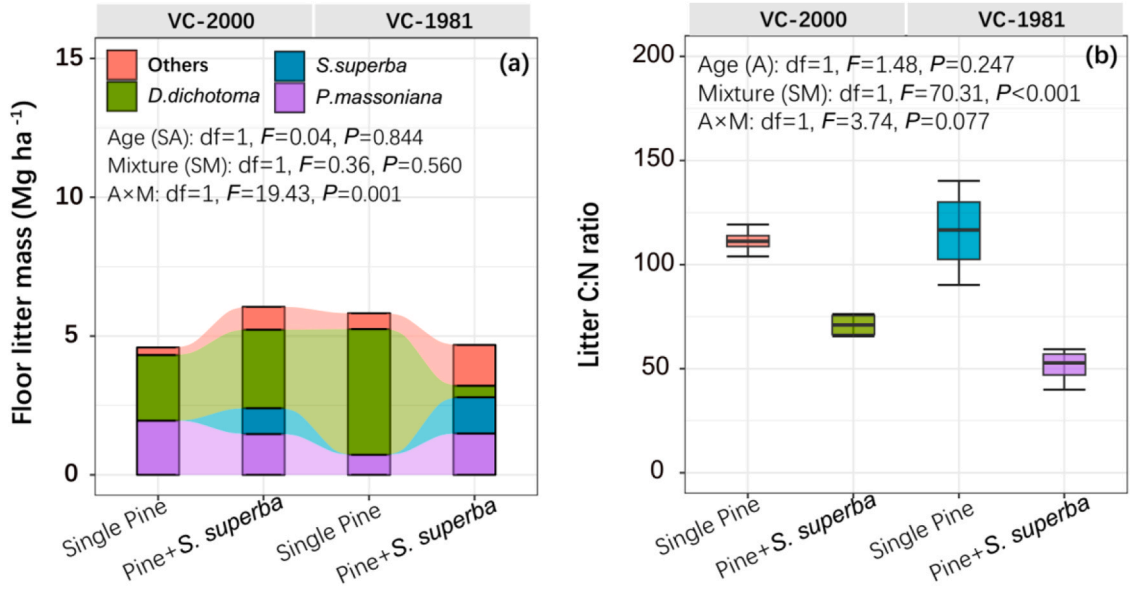


**Fig. 3.** Forest floor litter mass (a) and litter C:N ratio (b) in single pine and pine+*S. superba* plots in VC-2000 and VC-1981 stands. The effects of stand age (A), species mixture (M), and their interaction (A × M) were tested using the generalized linear model (GLM). VC-1981 and VC-2000 represent vegetation cover (VC) established in 1981 and 2000, respectively.

(Fig. 7ab). Notably, mixed plantation systems alleviated the constraints imposed by soil properties on microbial necromass accumulation that were observed in monoculture settings, while concurrently enhancing microbial functional diversity through strengthened CUE-bacterial necromass coupling ($P < 0.01$; Fig. S5 and S6).

## 4. Discussion

Our study delineates a dual-pathway mechanism governing SOC sequestration in mixed tree plantations, reconciling temporal dynamics of fungal and bacterial necromass contributions. We demonstrate that tree species mixing rapidly enhances fungal necromass accumulation—establishing foundational SOC pools—while bacterial necromass emerges as the dominant regulator of long-term SOC augmentation, challenging the fungal-centric paradigm of SOC formation. Crucially, mixed systems optimize microbial functional succession: early-stage fungal dominance facilitates recalcitrant organic matter decomposition through EcM network proliferation, while bacterial communities subsequently drive SOC stabilization via enhanced microbial CUE and diversity-mediated necromass preservation. These phased microbial interactions are tightly coupled to improved litter quality (reduced C:N ratios) and soil nutrient dynamics, revealing an overlooked synergy between substrate modification and microbial life-history strategies in steering SOC trajectories.

### 4.1. Rapid positive effect of tree species mixing on fungal necromass

Our findings confirm the first hypothesis that mixed pine-broadleaf plantations exhibit elevated bacterial and fungal necromass production alongside increased SOC stocks. Notably, stand age exerted significant effects on SOC stocks and bacterial necromass C, whereas fungal necromass C and total microbial necromass C remained age-insensitive. Fungal necromass C maintained stable concentrations across young and mature stands in both monoculture and mixed plantations, suggesting that fungal necromass accumulation exhibits a faster response to tree species mixing—a critical driver of SOC accrual. In contrast, bacterial necromass accumulation paralleled SOC stock dynamics, displaying a closer 1:1 correlation with SOC compared to fungal necromass. We therefore propose a dual-pathway framework: fungal necromass C establishes the baseline SOC pool, while bacterial necromass C governs subsequent SOC augmentation. These results challenge the prevailing paradigm emphasizing fungal necromass dominance in SOC formation under tree diversity or vegetation shifts (Wang et al., 2021; Hu et al., 2023; Angst et al., 2024), highlighting bacterial contributions as a previously underappreciated regulatory mechanism.

The accumulation of microbial necromass in forest soils is regulated by multiple interacting factors, including the quantity and quality of plant-derived inputs, microbial biomass, community diversity and metabolic efficiency, and soil nutrient dynamics (Whalen et al., 2022; Camenzind et al., 2023; Deng et al., 2023). Our findings demonstrate that tree species mixing significantly enhanced microbial biomass C while concurrently inducing a pronounced reduction in the fungal-to-bacterial (F:B) ratio, indicative of shifts in microbial community structure and functional dominance. Notably, fungal biomass exhibited no statistically significant response to either tree species mixing or stand age, whereas stand age emerged as a critical determinant of fungal diversity. These patterns collectively suggest that the rapid compositional changes in fungal necromass C observed under tree species mixing regimes are primarily mediated through fungal biomass dynamics, while fungal diversity exerts a secondary influence modulated by temporal lag effects.

Furthermore, the functional prediction analysis showed that tree species mixture significantly increased EcM fungi associated with no stand-age effects. This implies that the rapid EcM fungal proliferation and subsequent root network establishment drive fungal necromass C accrual in soils (Lladó et al., 2018; Coban et al., 2022) since there is only a strong positive relationship between EcM fungi and fungal necromass. In contrast, there were no significant changes in bacterial biomass; bacterial necromass C correlated more strongly with bacterial α-diversity than biomass, positioning bacterial necromass as the predominant predictor of SOC stocks.

### 4.2. Mixed tree species enhance microbial necromass by promoting microbial diversity and litter quality

The relative importance of litter quantity versus quality in influencing soil C cycling under tree species mixing has been extensively debated (Lyu et al., 2019; Chen et al., 2020; Hua et al., 2022; Deng et al., 2023). Our results demonstrate that while tree species mixing did not significantly increase aboveground litter production, it substantially

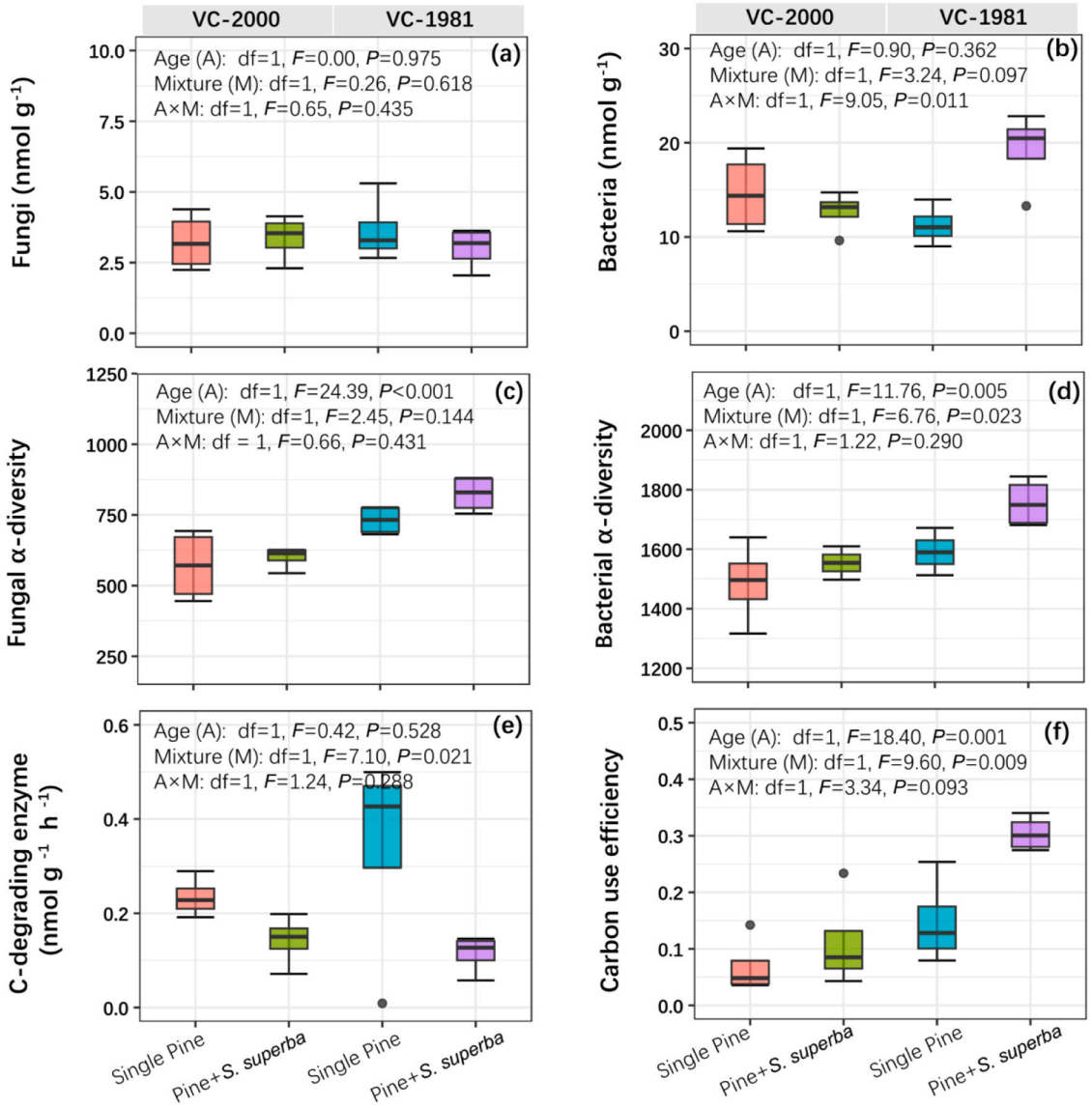


**Fig. 4.** Fungal (a) and bacterial (b) phospholipid fatty acids (PLFAs), fungal (c) and bacterial (d) α-diversity (Chao1 index), C-degrading enzyme (e) and microbial c utilization efficiency (CUE) (f) in single pine and pine+*S. superba* plots in VC-2000 and VC-1981 stands. The effects of stand age (A), species mixture (M), and their interaction (A × M) on, fungi, bacteria, fungal and bacterial α-diversity, C-degrading enzyme, and CUE with the test of significance of GLM. VC-1981 and VC-2000 represent vegetation cover (VC) established in 1981 and 2000, respectively.

reduced the litter C:N ratio, revealing that litter quality rather than quantity governs soil C accumulation. The strong negative correlations observed between litter C:N ratio and total microbial necromass (including both fungal and bacterial components) further support the premise that enhanced litter quality under mixed plantations promotes microbial necromass formation. The improved litter quality in mixed stands diversifies substrate availability and creates additional ecological niches for bacterial communities. This is evidenced by significantly increased bacterial diversity that shows strong associations with microbial necromass accumulation, particularly bacterial-derived necromass. Partial correlation analyses substantiate these relationships - controlling for litter C:N ratio (but not litter quantity) markedly reduced the strength of correlations between microbial diversity/metabolic traits and necromass accumulation. Similarly, accounting for soil N parameters (litter N pool, total N, and DON) significantly weakened the relationships between microbial properties and necromass. Our findings elucidate two distinct mechanisms driving necromass accumulation: For fungal necromass, mixing improves litter quality and soil N availability, stimulating extracellular matrix fungi proliferation and enhancing C-degrading enzyme activities. Bacterial necromass accumulation results from increased litter N content and reduced C:N ratios, which optimize bacterial CUE (Li et al., 2024), coupled with soil N enrichment (total N and DON) that enhances bacterial diversity and functional capacity

Notably, the accelerated necromass accumulation in mixed stands primarily stems from strengthened microbe-soil physicochemical interactions, with particularly pronounced effects on bacterial necromass. Partial Mantel tests verified significant influences of litter and soil properties on bacterial/fungal community structure and fungal functional potential, with tighter microbiome-environment coupling in mixed versus monoculture plantations (Allsup et al., 2023; Lyu et al., 2023). SEM indicates that mixed plantations enhance necromass contributions by mitigating soil physicochemical constraints on microbial activity. Whereas monoculture soils suppress necromass formation through accelerated biotic/abiotic decomposition, species mixing alleviates these limitations while fostering synergistic litter-soil interactions. Random forest analyses revealed particularly strengthened associations between bacterial necromass and integrated

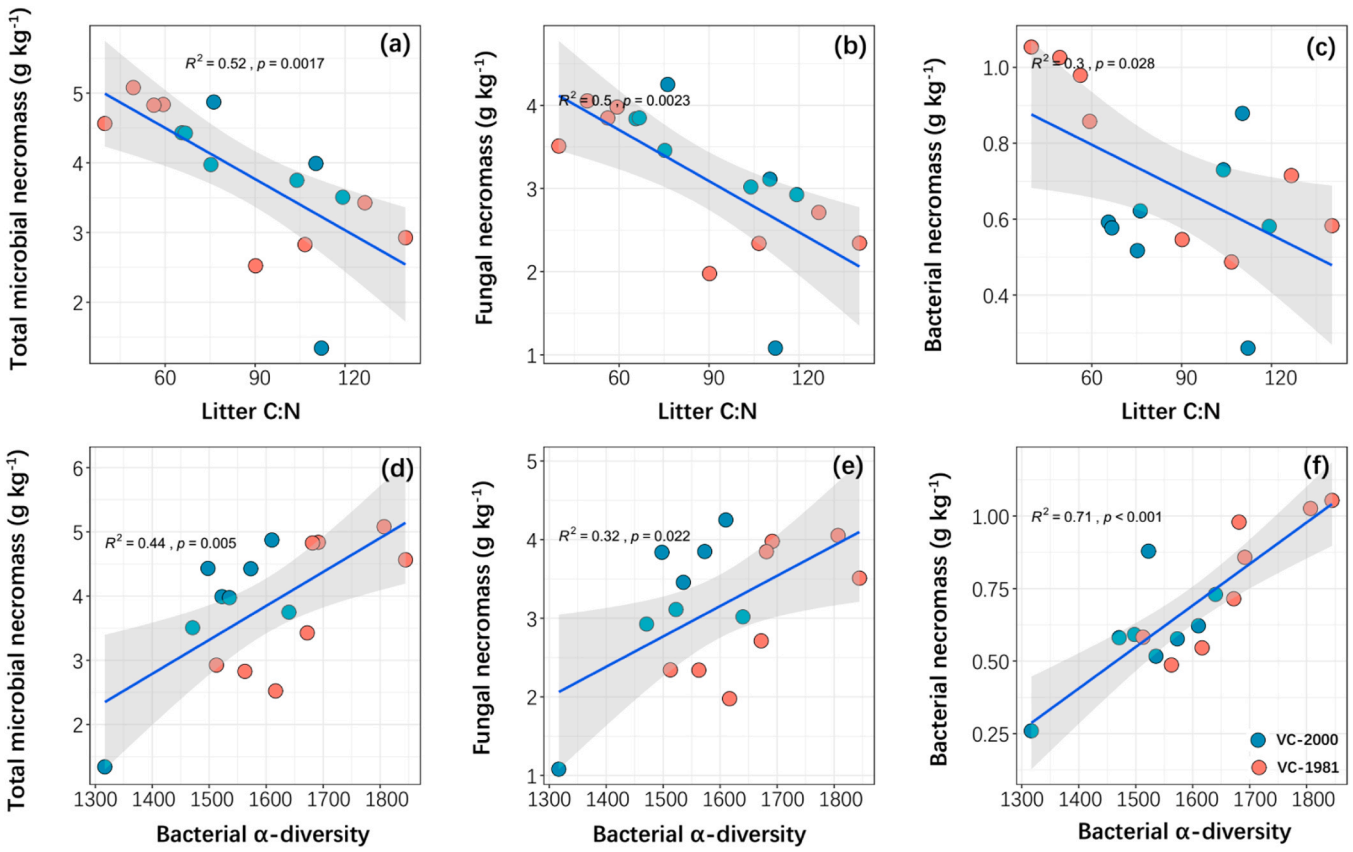


**Fig. 5.** Significant correlations exist between (a-c) litter C:N ratio and (d-f) bacterial α-diversity with total microbial necromass, fungal necromass, and bacterial necromass components. Gray bands indicate 95 % confidence intervals, with VC-1981 and VC-2000 representing vegetation cover established in 1981 and 2000, respectively.

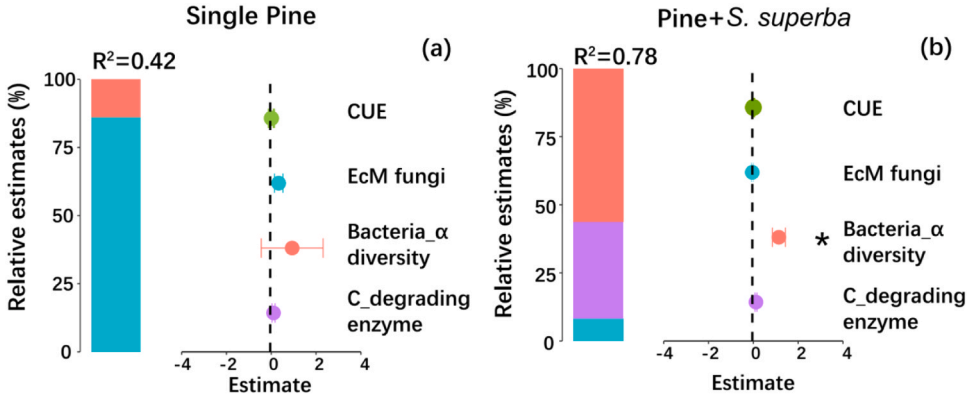


**Fig. 6.** The relative influence of multiple predictors on total microbial necromass in single pine (a), and pine+*S. superba* plots (b). the standardized regression coefficients for each predictor and their associated 95 % confidence intervals are shown. $r^2$ represents the proportion of variance explained by all predictors. *$p < 0.05$.

soil-litter-microbial dynamics. A key finding is that mixed plantations develop extensive EcM fungal networks with diversified root architectures, facilitating nutrient acquisition from recalcitrant organic matter and preferentially channeling resources into fungal necromass production. As nutrient availability improves, microbial communities transition toward bacterial-dominated states. Collectively, our results demonstrate that tree species mixing accelerates microbially-mediated SOM restoration in degraded ecosystems through fungal-dominated pathways.

### 4.3. Applications and consequences

This study uncovers a temporally staggered microbial relay mechanism underpinning SOC sequestration in degraded ecosystems restored through conifer-broadleaf mixtures. Crucially, we identify fungal necromass as the pioneer responder to tree species mixing during initial restoration phases, while bacterial necromass emerges as the sustained driver of long-term SOC stabilization—a dichotomy reflecting distinct life-history strategies between r-selected fungi and K-selected bacteria in fluctuating nutrient regimes. This functional succession enables a self-reinforcing C capture loop: early fungal dominance primes recalcitrant

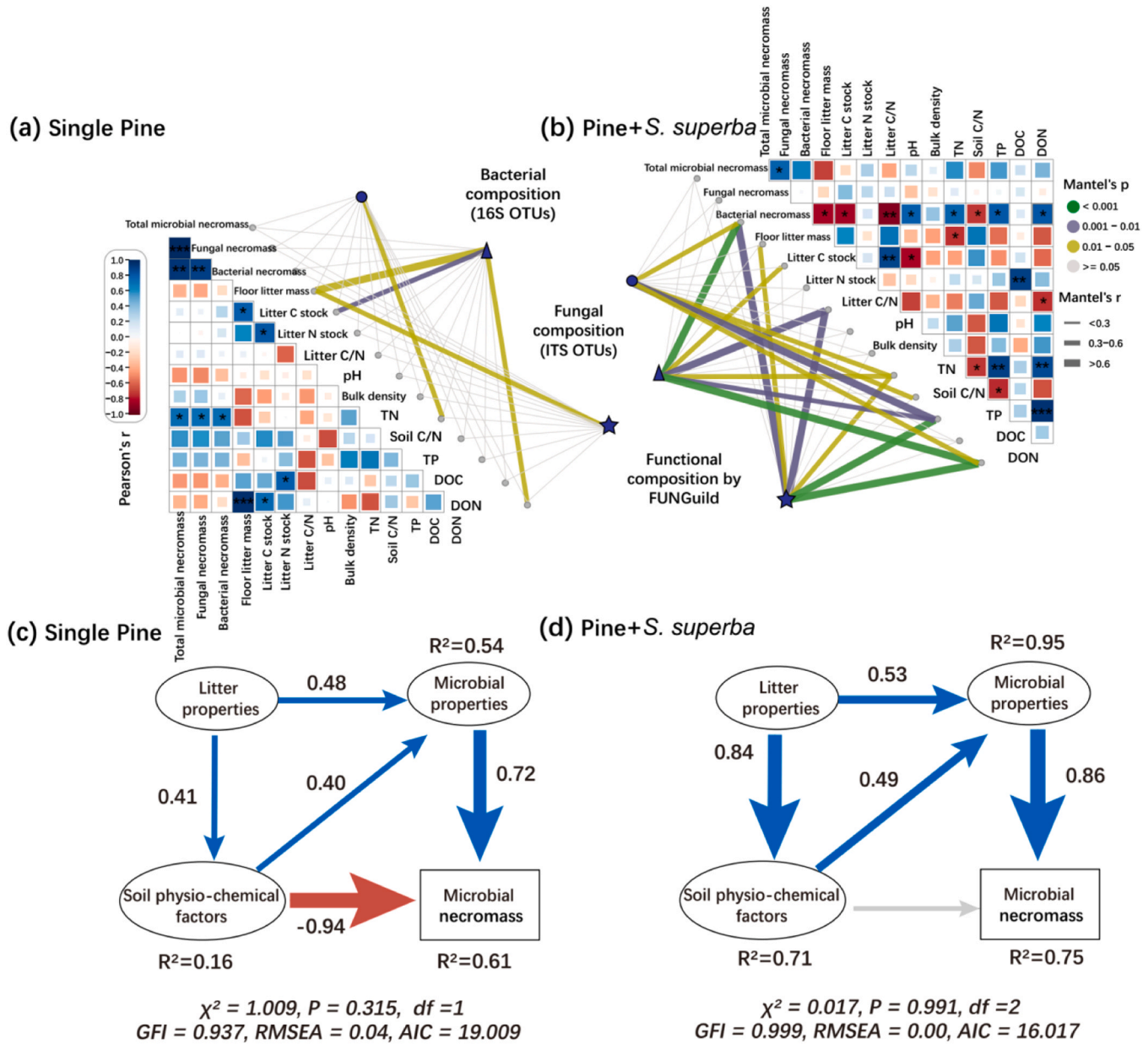


**Fig. 7.** Correlation between environmental variables and microbial community composition. The bacterial and fungal composition based on Bray-Curtis distance is related to each environmental factor (microbial necromass, litter, and soil physical and chemical properties) by partial mantel test in single pine (a) and in pine+*S. superba* plots (b). line width corresponds to the partial Mantel's r value, and line color denotes the statistical significance. The color of the blocks in the figure is based on based on pearson's correlation coefficients. Asterisks indicate statistical significance (***, $p < 0.001$; **, $p < 0.01$; *, $p < 0.05$). effects of litter properties, soil physio-chemical factors, and microbial composition on microbial necromass C in single pine (c) and pine+*S. superba* (d) plots by structural equation model. Blue arrows and red arrows indicate significantly positive and negative relationships, respectively. The arrow width is proportional to the strength of the relationship. Ellipse represents the first component from the principal component analysis, conducted for the litter properties (forest N stock, litter C:N), soil physio-chemical factors (TP, TN, soil bulk density, DON, DOC, pH, soil C:N), microbial properties (bacterial α-diversity, fungal α-diversity, fungi, bacteria).

organic matter decomposition, while later bacterial proliferation optimizes metabolic efficiency for necromass preservation.

Notably, our findings challenge the conventional view of microbial contributions as static by revealing phase-dependent functional complementarity between fungal and bacterial necromass. Broadleaf introduction creates niche cross-facilitation, where fungal-derived compounds selectively enrich bacterial taxa capable of stabilizing labile metabolites into mineral-associated SOC—a process amplified by the dual role of EcM fungi in both nutrient foraging and microbiome engineering.

These insights redefine restoration paradigms by positioning microbial functional succession as a keystone criterion for evaluating ecosystem recovery, helping to address critical gaps in current climate-smart restoration strategies, which often overlook microbial metacommunity dynamics when scaling up C sequestration projects. By mechanistically linking tree diversity to microbially mediated C cascades, this work provides actionable levers for precision restoration—targeted enrichment of EcM-host networks could accelerate early SOC accrual, while later-stage management might prioritize litter quality modulation to sustain bacterial necromass production. This temporal stratification of microbial engineering principles offers a blueprint for optimizing global C farming initiatives in anthropogenically altered landscapes.

## 5. Conclusion

This study investigated the mechanisms of soil C sequestration by comparing mixed Pine + *S. superba* plantations with single pine stands across different restoration stages in degraded lands. Our key findings demonstrate that tree species mixing drives a sequential microbial necromass accumulation pattern—initially enhancing fungal necromass production, which subsequently facilitates more stable bacterial necromass formation, ultimately promoting SOC accumulation. The superior performance of mixed plantations is attributed to three interconnected factors: Improved litter quality (lower C:N ratio), which optimizes substrate availability for microbial decomposition; Enhanced microbial functional traits, including: Increased bacterial α-diversity, higher EcM fungal abundance, elevated microbial CUE; Strengthened nutrient acquisition, where these microbial adaptations collectively accelerate necromass production through more efficient organic matter transformation. These results provide a mechanistic framework for understanding how mixed-species plantations enhance SOC storage in degraded forests. By elucidating these plant-microbe-soil interactions, our study offers science-based strategies for selecting species combinations and management approaches to maximize C sequestration during forest restoration. Future research should explore how these mechanisms vary across different soil types and climatic conditions to develop region-specific restoration protocols.

## CRediT authorship contribution statement

**Yusheng Yang:** Writing – review & editing. **Jinsheng Xie:** Writing – review & editing, Supervision, Methodology, Funding acquisition, Conceptualization. **Yuming Lu:** Investigation, Data curation. **Yongmeng Jiang:** Methodology, Investigation, Formal analysis. **Jordi Sardans:** Writing – review & editing. **Penuelas Josep:** Writing – review & editing, Conceptualization. **Maokui Lyu:** Writing – review & editing, Funding acquisition, Data curation, Conceptualization. **Cui Deng:** Writing – original draft, Investigation, Formal analysis, Data curation, Conceptualization.

## Declaration of Competing Interest

The authors declare no competing interests listed in this work.

## Acknowledgments

This research was funded by the National Natural Science Foundation of China (Nos. 32030073, 32471653, and 31870604) and the Special Project for Guiding Science and Technology Development of Local Government by the Central Government of China (No. 2022L3009). We thank Shiliang Zhang, Jiayu Li and Cong Cao for helping with laboratory and field work. We would like to acknowledge Prof. Yolima Carrillo at Western Sydney University and Prof. Guangshui Chen at Fujian Normal University for their contribution to this revision by enhancing the language clarity and scientific rigor throughout the manuscript. We would like to thank Dr. Daniel Petticord at the University of Cornell for his assistance with the English language and grammatical editing of the manuscript.

## Appendix A. Supporting information

Supplementary data associated with this article can be found in the online version at doi:10.1016/j.foreco.2025.122918.

## Data availability

The data that has been used is confidential.

## References

Adams, R.I., Miletto, M., Taylor, J.W., Bruns, T.D., 2013. Dispersal in microbes: fungi in indoor air are dominated by outdoor air and show dispersal limitation at short distances. ISME J. 7, 1262–1273. https://doi.org/10.1038/ismej.2013.28.

Allsup, C.M., George, I., Lankau, R.A., 2023. Shifting microbial communities can enhance tree tolerance to changing climates. Science 380 (6647), 835–840. https://doi.org/10.1126/science.adf2027.

Angst, G., Angst, Š., Frouz, J., Jabinski, S., Jílková, V., Kukla, J., Li, M., Meador, T.B., Angel, R., 2024. Stabilized microbial necromass in soil is more strongly coupled with microbial diversity than the bioavailability of plant inputs. Soil Biol. Biochem 190, 109323. https://doi.org/10.1016/j.soilbio.2024.10932.

Appuhn, A., Joergensen, R.G., 2006. Microbial colonisation of roots as a function of plant species. Soil Biol. Biochem 38 (5), 1040–1051. https://doi.org/10.1016/j.soilbio.2005.09.002.

Bai, Y., Zha, X., Chen, S., 2020. Effects of the vegetation restoration years on soil microbial community composition and biomass in degraded lands in changting county, China. J. For. Res. 31 (4), 1295–1308. https://doi.org/10.1007/s11676-019-00879-z.

Berthrong, S.T., Jobbágy, E.G., Jackson, R.B., 2009. A global meta-analysis of soil exchangeable cations, ph, carbon, and nitrogen with afforestation. Ecol. Appl. 19, 2228–2241. https://doi.org/10.1890/08-1730.1.

Breiman, L., 2001. Random forests. Mach. Learn. 45, 5–32. https://doi.org/10.1023/A:1010933404324.

Bukoski, J.J., Cook-Patton, S.C., Melikov, C., Ban, H., Chen, J.L., Goldman, E.D., Harris, N.L., Potts, M.D., 2022. Rates and drivers of aboveground carbon accumulation in global monoculture plantation forests. Nat. Commun. 13 (1), 1–13. https://doi.org/10.1038/s41467-022-31380-7.

Camenzind, T., Mason-Jones, K., Mansour, I., Rillig, M.C., Lehmann, J., 2023. Formation of necromass-derived soil organic carbon determined by microbial death pathways. Nat. Geosci. 16, 115–122. https://doi.org/10.1038/s41561-022-01100-3.

Cao, S., Zhong, B., Yue, H., Zeng, H., Zeng, J., 2009. Development and testing of a sustainable environmental restoration policy on eradicating the poverty trap in China's changting county. P. Natl. Acad. Sci. USA 106 (26), 10712. https://doi.org/10.1073/pnas.0900197106.

Caporaso, J.G., Kuczynski, J., Stombaugh, J., Bittinger, K., Bushman, F.D., Costello, E.K., Fierer, N., Peña, A.G., Goodrich, J.K., Gordon, J.I., Huttley, G.A., Kelley, S.T., Knights, D., Koenig, J.E., Ley, R.E., Lozupone, C.A., McDonald, D., Muegge, B.D., Pirrung, M., Reeder, J., Sevinsky, J.R., Turnbaugh, P.J., Walters, W.A., Widmann, J., Yatsunenko, T., Zaneveld, J., Knight, R., 2010. QIIME allows analysis of high-throughput community sequencing data. Nat. Methods 7 (5), 335–336. https://doi.org/10.1038/NMETH.F.303.

Chazdon, R.L., 2008. Beyond deforestation: restoring forests and ecosystem services on degraded lands. Science 320 (5882), 1458–1460. https://doi.org/10.1126/science.1155365.

Chen, L., Liu, L., Mao, C., Qin, S., Wang, J., Liu, F., Blagodatsky, S., Yang, G., Zhang, Q., Zhang, D., Yu, J., Yang, Y., 2018. Nitrogen availability regulates topsoil carbon dynamics after permafrost thaw by altering microbial metabolic efficiency. Nat. Commun. 9, 3951. https://doi.org/10.1038/s41467-018-06232-y.

Chen, X., Chen, H.Y., Chen, C., Ma, Z., Searle, E.B., Yu, Z., Huang, Z., 2020. Effects of plant diversity on soil carbon in diverse ecosystems: a global meta-analysis. Biol. Rev. 95 (1), 167–183. https://doi.org/10.1111/brv.12554.

Coban, O., De Deyn, G.B., van der Ploeg, M., 2022. Soil microbiota as game-changers in restoration of degraded lands. Science 375 (6584), abe0725. https://doi.org/10.1126/science.abe0725.

Deng, C., Lyu, M., Xiong, X., Peñuelas, J., Sardans, J., Li, X., Lin, W.S., Yang, Y.S., Xie, J., 2023. Understory ferns removal downregulates microbial carbon use efficiency and carbon accrual in previously degraded lands. Agric. For. Meteor. 340, 109631. https://doi.org/10.1016/j.agrformet.2023.109631.

Dick, W.A., Tabatabai, M.A., 1977. An alkaline oxidation method for determination of total phosphorus in soils. Soil Sci. Soc. Am. J. 41, 511–514. https://doi.org/10.2136/sssaj1977.03615995004100030015x.

Doetterl, S., Stevens, A., Six, J., Merckx, R., Van Oost, K., Casanova Pinto, M., Casanova-Katny, A., Muñoz, C., Boudin, M., Venegas, E.Z., Boeckx, P., 2015. Soil carbon storage controlled by interactions between geochemistry and climate. Nat. Geosci. 8 (10), 780–783. https://doi.org/10.1038/NGEO2516.

Edgar, R.C., 2013. UPARSE: highly accurate OTU sequences from microbial amplicon reads. Nat. Methods 10 (10), 996–998. https://doi.org/10.1038/NMETH.2604.

Feng, Y.H., Schmid, B., Loreau, M., Forrester, D.I., Fei, S.L., Zhu, J.X., Tang, Z.Y., Zhu, J. L., Hong, P.B., Ji, C.J., Shi, Y., Su, H.J., Xiong, X.Y., Xiao, J., Wang, S.P., Fang, J.Y., 2022. Multispecies forest plantations outyield monocultures across a broad range of conditions. Science 376 (6595), 865–868. https://doi.org/10.1126/science.abm6363.

Frostegård, Å., Tunlid, A., Bååth, E., 2011. Use and misuse of PLFA measurements in soils. Soil Biol. Biochem 43 (8), 1621–1625. https://doi.org/10.1016/j.soilbio.2010.11.021.

Gessner, M.O., Swan, C.M., Dang, C.K., McKie, B.G., Bardgett, R.D., Wall, D.H., Hattenschwiler, S., 2010. Diversity meets decomposition. Trends Ecol. Evol. 25, 372–380. https://doi.org/10.1016/j.tree.2010.01.010.

Hu, J., Du, M., Chen, J., Tie, L., Zhou, S., Buckeridge, K.M., Cornelissen, H.C., Huang, C., Kuzyakov, Y., 2023. Microbial necromass under global change and implications for soil organic matter. Glob. Change Biol. 29 (12), 3503–3515. https://doi.org/10.1111/gcb.16676.

Hua, F., Bruijnzeel, L.A., Meli, P., Martin, P.A., Zhang, J., Nakagawa, S., Miao, X., Wang, W., McEvoy, C., Peña-Arancibia, J.L., Brancalion, P.H.S., Smith, P., Edwards, D.P., Balmford, A., 2022. The biodiversity and ecosystem service

contributions and trade-offs of forest restoration approaches. Science 376 (6595), 839–844. https://doi.org/10.1126/science.abl4649.
Huang, Y., Chen, Y., Castro-Izaguirre, N., Baruffol, M., Brezzi, M., Lang, A., Li, Y., Härdtle, W., Oheimb, G., Yang, X., Liu, X., Pei, K., Both, S., Yang, B., Eichenberg, D., Assmann, T., Bauhus, J., Behrens, T., Buscot, F., Chen, X.Y., Chesters, D., Ding, B.Y., Durka, W., Erfmeier, A., Fang, J., Fischer, M., Guo, L.D., Guo, D., Gutknecht, J.L.M., He, J.S., He, C.L., Hector, A., Hönig, L., Hu, R.Y., Klein, A.M., Kühn, P., Liang, Y., Li, S., Michalski, S., Scherer-Lorenzen, S., Schmidt, K., Scholten, T., Schuldt, A., Shi, X., Tan, M.Z., Tang, Z., Trogisch, S., Wang, Z., Welk, E., Wirth, C., Wubet, T., Xiang, W., Yu, M., Yu, X.D., Zhang, J., Zhang, S., Zhang, N., Zhou, H.Z., Zhu, C.D., Zhu, L., Bruelheide, H., Ma, K., Niklaus, P.A., Schmid, B., 2018. Impacts of species richness on productivity in a large-scale subtropical forest experiment. Science 362 (6410), 80–83. https://doi.org/10.1126/science.aat6405.
Joergensen, R.G., 2018. Amino sugars as specific indices for fungal and bacterial residues in soil. Biol. Fertil. Soils 54 (5), 559–568. https://doi.org/10.1007/s00374-018-1288-3.
Jones, D.L., Willett, V.B., 2006. Experimental evaluation of methods to quantify dissolved organic nitrogen (DON) and dissolved organic carbon (DOC) in soil. Soil Biol. Biochem 38 (5), 991–999. https://doi.org/10.1016/j.soilbio.2005.08.012.
Lai, J.S, Zou, Y., Zhang, J.L., Pedro, R.P., 2022. Generalizing hierarchical and variation partitioning in multiple regression and canonical analyses using the rdacca.hp R package. Methods Ecol. Evol. 13 (4), 782–788.
Lal, R., Negassa, W., Lorenz, K., 2015. Carbon sequestration in soil. Curr. Opin. Environ. Sustain 15, 79–86. https://doi.org/10.1016/j.cosust.2015.09.002.
Lange, M., Eisenhauer, N., Sierra, C.A., Bessler, H., Engels, C., Griffiths, R.I., Mellado-Vázquez, P.G., Malik, A.A., Roy, J., Scheu, S., Steinbeiss, S., Thomson, B.C., Trumbore, S.E., Gleixner, G., 2015. Plant diversity increases soil microbial activity and soil carbon storage. Nat. Commun. 6 (1), 1–8. https://doi.org/10.1038/ncomms7707.
Li, S., Lyu, M., Deng, C., Deng, W., Wang, X., Cao, A., Jiang, Y., Liu, J., Lu, Y., Xie, J., 2024. Input of high-quality litter reduces soil carbon losses due to priming in a subtropical pine forest. Soil Biol. Biochem 194, 109444. https://doi.org/10.1016/j.soilbio.2024.109444.
Liang, C., Amelung, W., Lehmann, J., Kästner, M., 2019. Quantitative assessment of microbial necromass contribution to soil organic matter. Glob. Change Biol. 25 (11), 3578–3590. https://doi.org/10.1111/gcb.14781.
Lladó, S., López-Mondéjar, R., Baldrian, P., 2018. Drivers of microbial community structure in forest soils. Appl. Microbiol. Biotechnol. 102 (10), 4331–4338. https://doi.org/10.1007/s00253-018-8950-4.
Lu, Y., Lyu, M., Xiong, X., Deng, C., Jiang, Y., Zeng, M., Xie, J., 2023. Understory ferns promote the restoration of soil microbial diversity and function in previously degraded lands. Sci. Total Environ. 870, 161934. https://doi.org/10.1016/j.scitotenv.2023.161934.
Lü, M., Xie, J., Wang, C., Guo, J., Wang, M., Liu, X., Chen, Y., Chen, G., Yang, Y., 2015. Forest conversion stimulated deep soil c losses and decreased c recalcitrance through priming effect in subtropical China. Biol. Fertil. Soil 51 (7), 857–867. https://doi.org/10.1007/s00374-015-1035-y.
Lyu, M., Xie, J., Giardina, C.P., Vadeboncoeur, M.A., Feng, X., Wang, M., Ukonmaanahoe, L., Linf, T.C., Kuzyakovg, Y., Yang, Y., 2019. Understory ferns alter soil carbon chemistry and increase carbon storage during reforestation with native pine on previously degraded sites. Soil Biol. Biochem 132, 80–92. https://doi.org/10.1016/j.soilbio.2019.02.004.
Lyu, M., Homyak, P.M., Xie, J., Penuelas, J., Ryan, M.G., Xiong, X., Sardans, J., Lin, W., Wang, M., Chen, G., Yang, Y., 2023. Litter quality controls tradeoffs in soil carbon decomposition and replenishment in a subtropical forest. J. Ecol. 111, 2181–2193. https://doi.org/10.1111/1365-2745.14167.
Magoč, T., Salzberg, S.L., 2011. FLASH: fast length adjustment of short reads to improve genome assemblies. Bioinformatics 27 (21), 2957–2963. https://doi.org/10.1093/bioinformatics/btr507.
Margenot, A.J., Wade, J., 2023. Getting the basics right on soil enzyme activities: a comment on sainju et al. (2022). Agrosyst. Geosci. Environ. 6, e20405. https://doi.org/10.1002/agg2.20405.
Prommer, J., Walker, T.W., Wanek, W., Braun, J., Zezula, D., Hu, Y., Hofhansl, F., Richter, A., 2020. Increased microbial growth, biomass, and turnover drive soil organic carbon accumulation at higher plant diversity. Glob. Change Biol. 26 (2), 669–681. https://doi.org/10.1111/gcb.14777.
Saiya-Cork, K.R., Sinsabaugh, R.L., Zak, D.R., 2002. The effects of long-term nitrogen deposition on extracellular enzyme activity in an acer saccharum forest soil. Soil Biol. Biochem 34, 1309–1315. https://doi.org/10.1016/S0038-0717(02)00074-3.
Shao, P., Lynch, L., Xie, H., Bao, X., Liang, C., 2021. Tradeoffs among microbial life history strategies influence the fate of microbial residues in subtropical forest soils. Soil Biol. Biochem 153, 108112. https://doi.org/10.1016/j.soilbio.2020.108112.
Sinsabaugh, R.L., Turner, B.L., Talbot, J.M., Waring, B.G., Powers, J.S., Kuske, C.R., Moorhead, D.L., Follstad Shah, J.J., 2016. Stoichiometry of microbial carbon use efficiency in soils. Ecol. Monogr. 86, 172–189. https://doi.org/10.1890/15-2110.1.
Soil Survey Staff, 2014. Keys to Soil Taxonomy, twelfth ed. USDA, Natural Resources Conservation Service.
Vance, E.D., Brookes, P.C., Jenkinson, D.S., 1987. Microbial biomass measurements in forest soils: determination of kc values and tests of hypotheses to explain the failure of the chloroform fumigation-incubation method in acid soils. Soil Biol. Biochem 19, 689–696. https://doi.org/10.1016/0038-0717(87)90050-2.
Wang, B., An, S., Liang, C., Liu, Y., Kuzyakov, Y., 2021. Microbial necromass as the source of soil organic carbon in global ecosystems. Soil Biol. Biochem 162, 108422. https://doi.org/10.1016/j.soilbio.2021.108422.
Whalen, E.D., Grandy, A.S., Sokol, N.W., Keiluweit, M., Ernakovich, J., Smith, R.G., Frey, S.D., 2022. Clarifying the evidence for microbial-and plant-derived soil organic matter, and the path toward a more quantitative understanding. Glob. Change Biol. 28 (24), 7167–7185. https://doi.org/10.3969/10.1111/gcb.16413.
White, D.C., Davis, W.M., Nickels, J.S., King, J.D., Bobbie, R.J., 1979. Determination of the sedimentary microbial biomass by extractible lipid phosphate. Oecologia 40, 51–62. https://doi.org/10.1007/BF00388810.
Wu, M.H., Chen, S.Y., Chen, J.W., Xue, K., Chen, S.L., Wang, X.M., Chen, T., Kang, S.C., Rui, J.P., Thies, J.E., Bardgett, R.D., Wang, Y.F., 2021. Reduced microbial stability in the active layer is associated with carbon loss under alpine permafrost degradation. P. Nat. Acad. Sci. USA 118 (25), e2025321118. https://doi.org/10.1073/pnas.2025321118.
Xie, J., Guo, J., Yang, Z., Huang, Z., Chen, G., Yang, Y., 2013. Rapid accumulation of carbon on severely eroded red soils through afforestation in subtropical China. For. Ecol. Manag 300, 53–59. https://doi.org/10.1016/j.foreco.2012.06.038.
Xu, N., Tan, G., Wang, H., Gai, X., 2016. Effect of biochar additions to soil on nitrogen leaching, microbial biomass and bacterial community structure. Eur. J. Soil Biol. 74, 1–8. https://doi.org/10.1016/j.ejsobi.2016.02.004.
Zhang, X., Amelung, W., 1996. Gas chromatographic determination of muramic acid, glucosamine, mannosamine, and galactosamine in soils. Soil Biol. Biochem 28 (9), 1201–1206. https://doi.org/10.1016/0038-0717(96)00117-4.
Zhao, G., Mu, X., Wen, Z., Wang, F., Gao, P., 2013. Soil erosion, conservation, and eco-environment changes in the loess plateau of China. Land Degrad. Dev. 24 (5), 499–510. https://doi.org/10.1002/ldr.2246.